International Journal of Thermophysics, Vol. 11, No. 6, 1990

Effects of Infrared Detector Nonlinearity on Thermal Diffusivity Measurements Using the Flash Method

J. J. Hoefler[1] and R. E. Taylor[1]

Received November 21, 1989

When using an infrared detector to measure temperature changes as in the case of the flash technique, the effects of detector nonlinearity can have drastic effects on the experimental data. In the flash technique, the detector nonlinearity tends to shift the calculated half-time to larger values, resulting in underpredicted values of thermal diffusivity especially in experiments performed at room temperature. In order to predict the error in the diffusivity calculation, the nonlinear relationship between the detector signal and the temperature change was developed into a Taylor series expansion used in the flash technique's mathematical model. The nonlinear detector model proves to yield accurate correction factors for the presently calculated values of diffusivity. In order to utilize the model, it is necessary to estimate the maximum temperature rise of the back surface and the degree of detector nonlinearity.

KEY WORDS: detector nonlinearity; flash technique; infrared detector; thermal diffusivity.

1. INTRODUCTION

Initially developed by Parker et al. [1], the flash technique has become a widely accepted method for measuring the thermal diffusivity of various samples over wide ranges of temperatures. The technique was first introduced to measure the thermal diffusivity of homogeneous samples and has since been modified to incorporate heterogeneous samples, including those composed of multiple layers [2]. The data analysis has also been modified to include radiation losses and finite pulse time effects of the heating pulse [3–5].

[1] Thermophysical Properties Research Laboratory, Purdue University, West Lafayette, Indiana 47906, U.S.A.

0195-928X/90/1100-1099$06.00/0

The experimental technique utilizes a very short-duration pulse of energy to heat the front surface of a sample. The resulting back surface temperature rise is then measured using either a thermocouple or a radiation detector. Defining the half-time ($t_{1/2}$) as the time at which the back surface temperature has reached half of its maximum rise, the thermal diffusivity for a homogeneous sample can be calculated from the relation [1]

$$\alpha = 1.37 \frac{L^2}{\pi^2 t_{1/2}} \tag{1}$$

where L is the thickness of the sample and α is the thermal diffusivity. This relation was derived for one-dimensional heat conduction through a homogeneous layer without heat losses, following a Dirac heating pulse. The nondimensional back surface temperature rise is shown in Fig. 1 with its x axis in number of half-times.

The method used to measure the temperature transient of the back surface is typically a thermocouple or a radiation detector. In many situa-

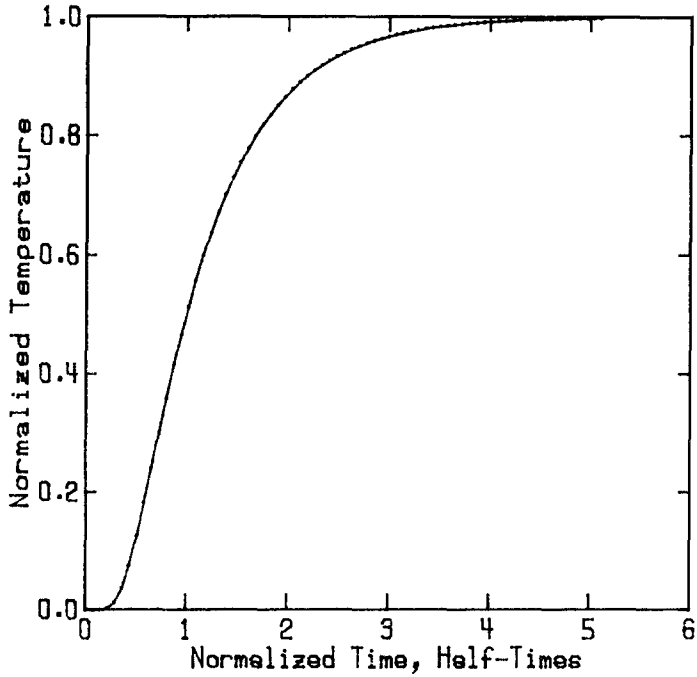

Fig. 1. Normalized rear surface temperature rise following an instantaneous heat pulse applied to the front surface.

tions, a radiation detector is more convenient to use than a thermocouple; thus it is necessary to have a relationship between the sample's back surface temperature and the infrared detector's output signal.

In the past, an infrared detector's output was approximated as linear to the temperature at which it was viewing. This approximation is fairly accurate for small temperature excursions at higher-temperature experimental operating conditions. Unfortunately, the linear approximation becomes very inaccurate for experiments performed at room temperature. Nonlinearity detector effects have been found to occur in as small as a 0.5-K rise at room temperature [6].

As first pointed out by Taylor et al [7, 8], the effect of detector nonlinearity on the flash technique is a tendency to predict lower values of diffusivity than expected [7–10]. Examining Eq. (1), the implication of this fact is that the calculated $t_{1/2}$ is larger than would be expected if the detector response was linear. For the situation of heterogeneous samples, the same results occur except the diffusivity is an effective diffusivity and the half-time is an effective half-time [2].

The objective of this work is to develop the mathematical relationship between the viewed temperature and the output of the detector. As will be shown, this is a very important consideration for experiments performed at room temperature.

2. MATHEMATICAL ANALYSIS OF MODEL

2.1. Rear Surface Temperature Rise of a Homogeneous Sample

The general solution for the back surface rise following an instantaneous heating pulse to the front surface, with an initial temperature of zero, can be written as [1]

$$T(L, t) = \frac{Q}{\rho C_p L}\left[1 + 2\sum_{n=1}^{\infty}(-1)^n \exp\left(\frac{-n^2\pi^2}{L^2}\alpha t\right)\right] \tag{2}$$

where

$Q \equiv$ energy content of the Dirac pulse
$\rho \equiv$ density of the sample material
$C_p \equiv$ specific heat of the sample
$L \equiv$ sample thickness
$k \equiv$ thermal conductivity of the sample
$\alpha \equiv k/\rho C_p \equiv$ thermal diffusivity of the sample

In order to eliminate the parameter Q from Eq. (2), the following calorimetric relation is used:

$$Q = \rho C_p L T_{\max} \tag{3}$$

where $T_{\max}$ represents the maximum temperature rise of the back surface. Defining the sample Fourier number as

$$\mathrm{FO} = \frac{\alpha t}{L^2} \tag{4}$$

Eq. (2) can then be written as

$$T(L, t) = T_{\max}\left[1 + 2\sum_{n=1}^{\infty}(-1)^n \exp(-n^2\pi^2 \mathrm{FO})\right] \tag{5}$$

Equation (5) can then be written in terms of dimensionless temperature simply as

$$\frac{T(L, t)}{T_{\max}} = \left[1 + 2\sum_{n=1}^{\infty}(-1)^n \exp(-n^2\pi^2 \mathrm{FO})\right] \tag{6}$$

From Eq. (6), the value of π^2FO is equal to 1.37 when the normalized temperature is 0.5. Combining this fact with Eq. (4), the relation given by Eq. (1) can easily be shown.

Equation (6) is very useful in that the exact units of temperature are not important; thus provided the device used to measure the experimental temperature transient produces a response which is linear to the temperature, the exact magnitude and units are arbitrary. Unfortunately, when an infrared detector is used to measure the transient, the approximation of linear response to temperature is extremely limited [7–10]. The following analysis will provide the relationship between an infrared detector's response and the actual temperature transient the detector is measuring.

2.2. Detector Response to a Change in Temperature

An infrared detector measures the intensity of emitted photons with a certain bandwith of infrared wavelengths. As the temperature of the film surface changes, the intensity of the emitted photons in the range of the detector's bandwidth also changes, resulting in a change in the detector's voltage output. Thus the voltage output must be related to the corresponding surface heat flux associated with the surface temperature.

The energy emitted by a body at a given temperature and wavelength is defined by Planck's distribution law, which states [11]

$$e_{b\lambda} = \frac{c_1 \lambda^{-5}}{\exp(c/\lambda) - 1} \tag{7}$$

where

$e_{b\lambda} \equiv$ spectral emittant energy of a blackbody
$\lambda \equiv$ wavelength (μm)
$T \equiv$ absolute temperature (K)
$c_1 \equiv 2\pi hc^2 = 3.74412 \times 10^8$ W $\cdot$ μm$^4 \cdot$ m^{-2}
$c_2 \equiv hc/k = 1.439 \times 10^4$ μm $\cdot$ K
$h \equiv$ Planck's constant
$k \equiv$ Boltzmann's constant
$c \equiv$ velocity of light in a vacuum

The wavelength at which maximum emission occurs can be found by differentiating Eq. (7) with respect to λ and setting the derivative to zero. This results in Wien's displacement law, which is given by [11]

$$\lambda_m T = 2897.76 \ \mu\text{m} \cdot \text{K} \tag{8}$$

Because the infrared detector has a limited spectrum from which it can optically view the sample's emitted energy, it is necessary to obtain a relation for the change in emitted energy, at the detector's bandwidth, due to a change in the film surface temperature. The development begins by defining the following two parameters [6, 12]:

$$n = \frac{T}{e_{b\lambda}} \left(\frac{\partial e_{b\lambda}}{\partial T} \right) \tag{9}$$

and

$$\Lambda = \frac{\lambda}{\lambda_m} \tag{10}$$

where n is the dimensionless sensitivity of the emitted energy at a specific wavelength with respect to an infinitesimal change in temperature, and Λ is the ratio of the center of the detector's infinitesimal bandwidth and the sample's maximum emission wavelength. By separating the variables in Eq. (9) and integrating, the spectral energy emitted at the sensitive wavelength of the detector can be written as [12]

$$e_{b\lambda} = KT^n \tag{11}$$

where K is the constant of integration. Using Planck's distribution and Eq. (9), it can be shown that the value of n approaches the following two asymptotic values [6]:

$$n \cong \frac{5}{\Lambda} \qquad \text{for} \quad \Lambda \leqslant 2.5 \tag{12a}$$

$$n \cong \frac{2.5}{\Lambda} + 1 \qquad \text{for} \quad \Lambda > 2.5 \tag{12b}$$

The greatest error in the approximations given by Eqs. (12a) and (12b) is 16% for $\Lambda = 2.5$ [6].

Because the detector is actually measuring measuring the emitted energy, Eq. (11) can be applied directly, noting that the constant K must also include the emissivity of the sample. Rewriting Eq. (11) in terms of the detector voltage result in

$$E = CT^n \tag{13}$$

where E is the detector voltage output, T is the actual surface temperature, and C and n are constants. The constant C depends on many factors such as the film emissivity, the voltage sensitivity of the detector, and the angular aperture of the detector [12, 13].

Performing a Taylor series expansion on Eq. (13), the voltage change as a function of temperature change can be written as [12]

$$E - E_0 = nCT_0^{n-1}(\Delta T) + \frac{n^2}{2!} CT_0^{n-2}(\Delta T)^2 + \cdots + \frac{n^n}{n!} C(\Delta T)^n \tag{14}$$

where ΔT is the temperature excursion, $T - T_0$. If the maximum temperature rise, $\Delta T_{\max}$, is much smaller than the initial temperature, T_0, Eq. (14) can be approximated as [12, 13]

$$E - E_0 \cong nCT^{n-1}(T - T_0) \tag{15}$$

Combining Eqs. (14) and (15), the percentage error in Eq. (9) due to the truncation of the series can be written as [12]

$$\varepsilon = \frac{\left[\frac{1}{2!}\left(\frac{n\,\Delta T}{T_0}\right) + \frac{1}{3!}\left(\frac{n\,\Delta T}{T_0}\right)^2 + \cdots + \frac{1}{n!}\left(\frac{n\,\Delta T}{T_0}\right)^{n-1}\right.}{\left.1 + \frac{1}{2!}\left(\frac{n\,\Delta T}{T_0}\right) + \frac{1}{3!}\left(\frac{n\,\Delta T}{T_0}\right)^2 + \cdots + \frac{1}{n!}\left(\frac{n\,\Delta T}{T_0}\right)^{n-1}\right]} \times 100 \tag{16}$$

Figure 2 shows a plot of Eq. (16) for various initial temperature conditions using an infrared detector with an infinitesimal bandwidth centered at 4 μm. Excluding the effects of a finite bandwidth, this wavelength is representative of the InSb detectors used in this work.

Observing Fig. 2, it is quite evident that experiments performed at room temperature yield significant errors for even small temperature excursions. Detector nonlinearity has been shown experimentally to have effects on room temperature measurements for as little as 2-K excursions [9]. However, excursions as large as 50 K at an ambient temperature of 900 K yield less than 20% error. By examining both Fig. 2 and Eq. (16), it is evident that high initial ambient temperatures are advantageous due to both thye reduction in n and the increase in T_0. The reduction in n is a result of the peak emission wavelength being shifted to lower values as a consequence of Wien's displacement law given by Eq. (8).

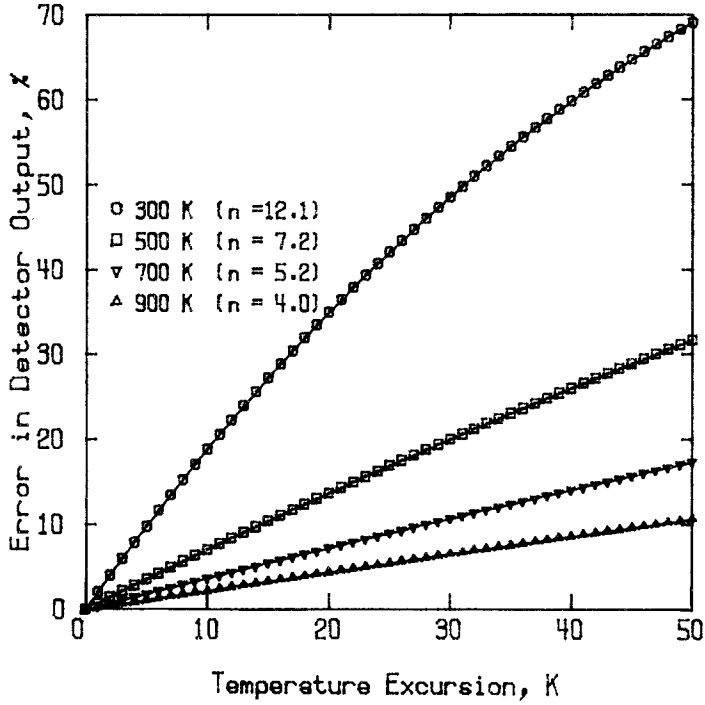

Fig. 2. Percentage error in the detector output due to the assumption of a linear detector response for a detector operating wavelength of 4.0 μm. Source: Hoefler [12].

2.3. Detector Nonlinearity Applied to the Flash Technique

In the typical flash technique, Eq. (15) is implicitly used in its normalized form. Specifically, the detector's voltage output is divided by the maximum voltage output, allowing for the constants in Eq. (15) to cancel and resulting in the following assumed linear relationship:

$$\frac{\Delta E(t)}{\Delta E_{\max}} = \frac{\Delta T(t)}{\Delta T_{\max}} \tag{17}$$

The relationship given by Eq. (17) is extremely limited in accuracy, as Fig. 2 indicates. The optimal conditions are obviously high temperatures with small temperature rises. The experiments performed at room temperature are extremely sensitive to any temperature excursions. Nonlinearity effects can occur with temperature rises as low as 0.5 K at room temperature [9].

In order to demonstrate graphically the effects of detector nonlinearity on the normalized curve, Eq. (5) was used to generate the actual

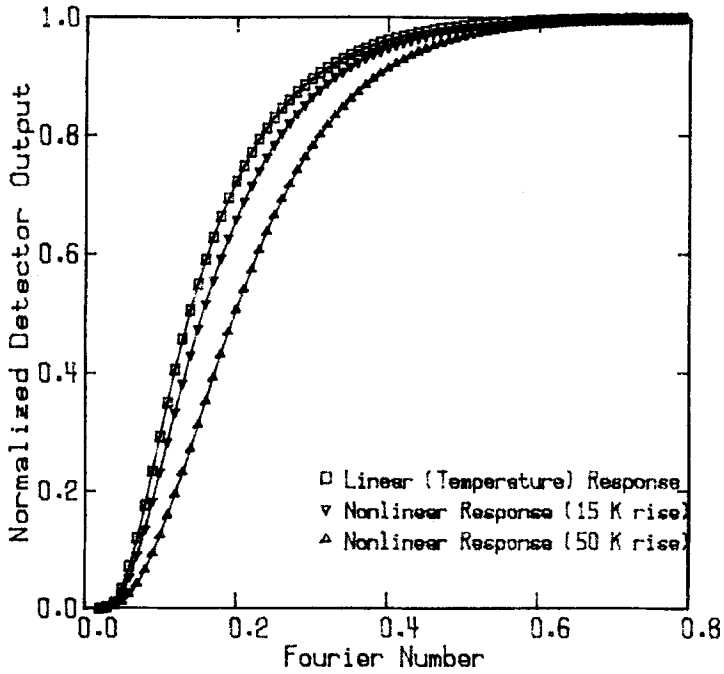

Fig. 3. Effect of a nonlinear detector response on the normalized rear surface temperature curve for an experimental operating temperature of 300 K.

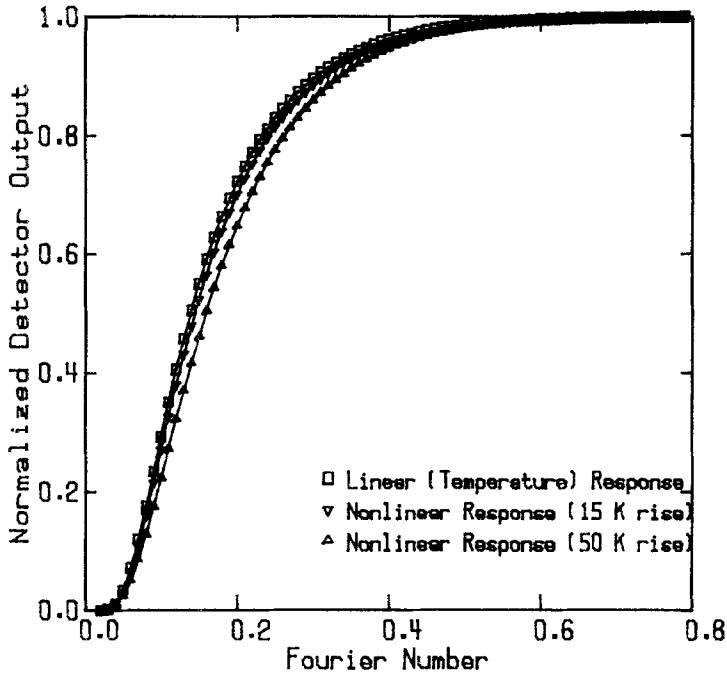

Fig. 4. Effect of a nonlinear detector response on the normalized rear surface temperature curve for an experimental operating temperature of 500 K.

temperature response for a given T_{max}. The calculated temperatures were then inserted into Eq. (14) to generate the theoretical nonlinear detector signals. This was done for ambient conditions of 300 and 500 K with the corresponding values of n calculated from Eqs. (8), (10), and (12a). The results are shown in Figs. 3 and 4. Both the figures show that the effect of nonlinearity is to shift the normalized curve to the right, resulting in an overpredicted value of $t_{1/2}$ or an underpredicted value of the thermal diffusivity. Table I gives the percentage error of the calculated $t_{1/2}$ for various ambient temperatures and T_{max}. From Table I it is obvious that a 5-K rise at room temperature yields the same error as a 50-K rise at 900 K.

3. EXPERIMENTAL RESULTS

In order to demonstrate the effects of detector nonlinearity, effective diffusivities were obtained for carbon-bonded carbon fiber samples (CBCF) [14, 15]. The transient temperature was determined using an InSb liquid nitrogen-cooled detector for various levels of laser power. Simultaneous back surface temperature rises were determined using a thermocouple in

Table I. Percentage Error in the Half-Time and the Diffusivity Calculated from the Half-Time, Due to a Nonlinear Detector Operating with a Wavelength of 4.0 μm[a]

ΔT_{max} (K)	$T_0 = 300$ K ($n = 12.1$)		$T_0 = 500$ K ($n = 7.2$)		$T_0 = 700$ K ($n = 5.2$)		$T_0 = 900$ K ($n = 4.0$)	
	α	$t_{1/2}$	α	$t_{1/2}$	α	$t_{1/2}$	α	$t_{1/2}$
2	−0.8	0.8	−0.1	0.1	−0.0	0.0	−0.0	0.0
5	−3.1	3.2	−0.7	0.7	−0.1	0.1	−0.0	0.0
10	−6.8	7.3	−2.0	2.1	−0.7	0.7	−0.1	0.1
15	−10.3	11.4	−3.4	3.5	−1.4	1.4	−0.5	0.5
20	−13.6	15.7	−4.7	4.9	−2.1	2.2	−1.0	1.0
30	−19.6	24.4	−7.3	7.9	−3.5	3.6	−1.8	1.8
40	−24.9	33.2	−9.8	10.8	−4.8	5.1	−2.7	2.7
50	−29.5	41.8	−12.2	13.9	−6.2	6.6	−3.5	3.6

[a] The values of n were calculated from Eqs. (8), (10), and (12a).

order to see the effect of ΔT_{max} on the experimentally calculated values of diffusivity. The effective diffusivity was calculated from Eq. (1) following heat loss corrections to the data. Overall, the experiments were performed at four separate ambient temperature conditions [14].

The theoretical value of diffusivity for each ambient condition was determined by extrapolating the data to the limit of $\Delta T_{max} \to 0$. The third column in Table II shows the experimentally calculated values of diffusivity with the exception of the values shown in parentheses, which are the extrapolated values. The fourth column gives the percentage error in the calculated diffusivity with respect to the extrapolated value. The fifth column gives the percentage error anticipated using Eqs. (6), (8), (10), (12a), and (14).

In order to determine the operating wavelength of the detector, the sensitivity curve as a function of wavelength was used [16]. The center wavelength used was that which corresponded to the area-weighted sensitivity band. In order words, the wavelength at which the area under the sensitivity curve left of the wavelength equaled the area under the sensitivity curve right of the wavelength was determined as the effective center wavelength. For the case of a liquid nitrogen-cooled InSb detector, this corresponded to approximately 4.0 μm.

The results indicated by Table II clearly show the effects of nonlinearity as ΔT_{max} increases or as T_0 decreases. The errors predicted from the nonlinear detector analysis agree quite well with the errors calculated from the experimental data.

Table II. Comparison of Calculated Diffusivity Errors from Experimental Data and That Predicted from the Analysis for Carbon-Bonded Carbon Fiber Samples[a]

T_0 (K)	ΔT_{max} (K)	Diffusivity ($cm^2 \cdot s^{-1}$)	% error in diffusivity[b]	% error predicted[c]
296	$\Delta T_{max} \to 0$	(0.00425)[d]	0.00	0.00
	1.2	0.00422	−0.71	−0.21
	6.7	0.00402	−5.41	−4.50
	9.5	0.00393	−7.52	−6.60
	17.0	0.00368	−13.41	−11.87
	41.0	0.00315	−25.88	−25.84
373	$\Delta T_{max} \to 0$	(0.00395)[d]	0.00	0.00
	4.9	0.00385	−2.52	−1.78
	8.4	0.00380	−3.72	−3.40
	12.4	0.00370	−6.26	−5.64
	30.0	0.00342	−13.25	−13.15
473	$\Delta T_{max} \to 0$	(0.00368)[d]	0.00	0.00
	0.6	0.00368	0.00	0.00
	3.4	0.00361	−1.90	−1.14
	9.0	0.00356	−3.26	−2.81
573	$\Delta T_{max} \to 0$	(0.00342)[d]	0.00	0.00
	0.5	0.00342	0.00	0.00
	2.7	0.00342	0.00	0.00
	3.8	0.00340	−0.58	−0.06
	6.9	0.00340	−0.58	−0.71

[a] Experimental data from Groot [14].
[b] Error in the experimentally calculated diffusivity assuming the correct value is the extrapolated value.
[c] Error in diffusivity predicted from nonlinear detector analysis assuming a detector operating wavelength of 4.0 μm.
[d] Extrapolated value of data as $\Delta T_{max} \to 0$.

4. CONCLUSIONS

The effect of detector nonlinearity on the calculation of thermal diffusivity from experimental data can be large, especially at room temperature and below. The approach of developing the Taylor series expansion on the nonlinear relationship between the detector output and the surface temperature provides an accurate description of the nonlinear detector effects on the flash technique. The nonlinear detector model can accurately predict the error in the calculation of diffusivity from the experimental data due to nonlinear detector operation provided the maximum temperature rise on the back surface is known, and the effective operating wavelength of the detector can be estimated.

REFERENCES

1. W. J. Parker, R. J. Jenkins, C. P. Butler, and G. L. Abbott, *J. Appl. Phys.* **32**:1679 (1961).
2. R. E. Taylor and K. D. Maglić, in *Compendium of Thermophysical Property Measurement Methods, Vol. I*, K.D. Maglić, A. Cezairliyan, and V. E. Peletsky, eds. (Plenum Press, New York, 1984), pp. 305–336.
3. L. M. Clark III and R. E. Taylor, *J. Appl. Phys.* **46**:4584 (1975).
4. R. C. Heckman, *J. Appl. Phys.* **44**:1455 (1973).
6. M. G. Dreyfus, *Appl. Opt.* **2**(11):1113 (1963).
5. R. E. Taylor and L. M. Clark III, *High Temp. High Press.* **6**:65 (1974).
7. R. E. Taylor, H. Groot, and R. L. Shoemaker, in *17 Biennial Conference on Carbon*, University of Kentucky, Lexington (1985).
8. R. E. Taylor, in *Thermal Conductivity, Vol. 19*, D. W. Yarbrough, ed. (Plenum Press, New York, 1988), pp. 407–409.
9. D. P. H. Hasselman and K. Y. Donaldson, *Int. J. Thermophys.* (in press).
10. D. P. H. Hasselman and G. Mekel, *J. Am. Ceram. Soc.* **72**:967 (1989).
11. R. Siegel and J. R. Howell, *Thermal Radiation Heat Transfer* (McGraw–Hill, New York, 1981), Chaps. 2 and 13.
12. J. J. Hoefler, M.S.M.E. thesis (Purdue University, West Lafayette, Ind., Dec. 1989), Chap. 2, App. B.
13. P. Cielo, *J. Appl. Phys.* **56**:230 (1984).
14. H. Groot, in *Thermal Conductivity, Vol. 20*, D. P. H. Hasselman and J. R. Thomas, Jr., eds. (Plenum Press, New York, 1989), pp. 361–363.
15. G. C. Wei and J. M. Robbins, *Bull. Am. Ceram. Soc.* **64**:691 (1985).
16. W. D. Lawson and J. W. Sabey, in *Research Techniques in Nondestructive Testing, Vol. I*, R. S. Sharpe, ed. (Academic Press, New York, 1970), pp. 443–454.